

# A Barometric Exponential Model of the Atmosphere's Refractive Index: Zenith Angles and Second Order Aberration in the Entrance Pupil

Richard J. Mathar\*

*Max-Planck Institute of Astronomy, Königstuhl 17, 69117 Heidelberg, Germany*

(Dated: April 27, 2020)

This report models the refractive index above a telescope site by a homogeneous atmosphere with exponential decay of the refractive index (susceptibility) as a function of altitude. The air is represented as a spherical hull with a symmetry center at the Earth center. We compute (i) the differential zenith angle — the difference between the actual zenith angle at arrival of rays at the telescope and a hypothetical zenith angle without the atmosphere — and (ii) the optical path length distribution of rays at arrival in the entrance pupil as a function of the distance to the pupil center.

The key technique of the semi-numerical mathematics in this work is to expand some integrals — that depend on the refractive index profile along the curved path of each ray from some virtual plane in the direction of the star up to the entrance pupil — in power series of small parameters.

## I. SPHERICAL SYMMETRY OF THE ATMOSPHERIC HULL

In ground-based astronomy, light emitted by astronomical objects is tilted more toward the zenith axis when arriving at the telescope than computed by standard spherical astronomy; the atmosphere acts like a gradient lens, and the actual zenith angle of arrival  $z_0$  differs from the astrometric zenith angle  $z$  of a hypothetical Earth in vacuum by an angle

$$R = z - z_0. \quad (1)$$

Figure 1 sketches the relevant variables. Applying successively Fresnel equations as light changes its direction when it encounters gradients in the refractive index  $n$ , the angle  $R$  is a functional of the refractive index along the path [1–7]

$$R = \rho n_0 \sin z_0 \int_1^{n_0} \frac{dn}{n \sqrt{r^2 n^2 - \rho^2 n_0^2 \sin^2 z_0}} \quad (2)$$

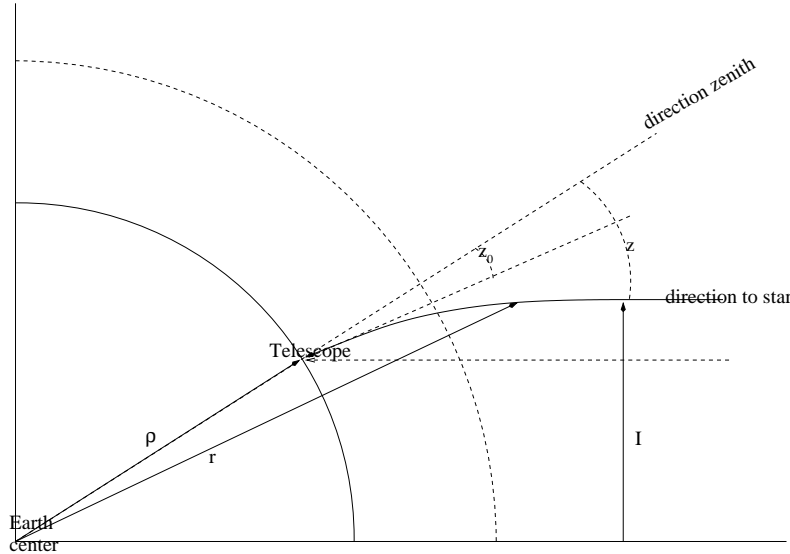


FIG. 1. Distance  $\rho$  of the telescope to the Earth center, distance  $r$  of a point on the curved path of the ray, true zenith angle  $z_0$ , astrometric zenith angle  $z$ , and impact parameter  $I$ . Not to scale.

\* <https://www.mpia-hd.mpg.de/homes/mathar>

measured in radians.  $\rho \approx 6378$  km is the radius of the Earth representing the curvature of the atmosphere above the telescope [8].  $n(r)$  is the refractive index at a distance  $r \geq \rho$  to the Earth center (!); it equals unity high above the atmosphere and increases to  $n_0 > 1$  at the telescope's altitude.

Evaluating  $R$  is a key to faithful pointing models and all-sky mapping of astrometry. Inserting wavelength-dependent refractive indices  $n$  leads to designs of atmospheric dispersion correctors.

We start from the Taylor expansion of  $R$  in odd powers of the tangent of the observed zenith angle [9],

$$R \equiv \sum_{i=1,3,5,7,\dots} \gamma_i \tan^i z_0, \quad (3)$$

such that [10]

$$\gamma_1 = \rho n_0 \int_1^{n_0} \frac{1}{n^2 r} dn; \quad (4)$$

$$\gamma_3 = \frac{1}{2} \rho n_0 \int_1^{n_0} \frac{\rho^2 n_0^2 - r^2 n^2}{n^4 r^3} dn; \quad (5)$$

$$\gamma_5 = \frac{3}{8} \rho n_0 \int_1^{n_0} \frac{(\rho^2 n_0^2 - r^2 n^2)^2}{n^6 r^5} dn; \quad (6)$$

$$\gamma_7 = \frac{5}{16} \rho n_0 \int_1^{n_0} \frac{(\rho^2 n_0^2 - r^2 n^2)^3}{n^8 r^7} dn; \quad (7)$$

$$\gamma_i = \binom{i-1}{\lfloor i/2 \rfloor} \frac{1}{4^{\lfloor i/2 \rfloor}} \rho n_0 \int_1^{n_0} \frac{(\rho^2 n_0^2 - r^2 n^2)^{\lfloor i/2 \rfloor}}{n^{i+1} r^i} dn. \quad (8)$$

## II. EXPONENTIAL REFRACTIVITY OF ALTITUDE

The first theme of this manuscript is to derive manageable formulas for the coefficients  $\gamma_i$  by introducing an exponential model of the refractive index  $n(r)$  as a function of altitude [11, 12]. The refractive index is related to the susceptibility  $\chi$  via

$$n(r) = \sqrt{1 + \chi(r)} \quad (9)$$

and we assume that the susceptibility is essentially proportional to an air density of scale height  $K$  such that

$$\chi(r) = \chi_0 e^{-(r-\rho)/K}. \quad (10)$$

At typical altitudes of observatories the susceptibility at the telescope is  $\chi_0 \approx 4 \times 10^{-4}$ , and the Earth atmosphere has a scale height  $K \approx 9.6$  km.

With such an explicit refractive index profile we switch from refractive indices to dimensionless altitudes  $\zeta \equiv (r - \rho)/K$  in the previous integrals:

$$\frac{dn}{d\zeta} = \frac{1}{2n} \frac{d\chi}{d\zeta}, \quad (11)$$

$$\frac{d\chi}{d\zeta} = -\chi(\zeta), \quad (12)$$

and substitute the variables in the integrals of the previous chapter:

$$\gamma_1 = \rho n_0 \int_0^\infty \frac{1}{n^2(\rho + \zeta K)} \frac{1}{2n} \chi(\zeta) d\zeta; \quad (13)$$

$$\gamma_3 = \rho n_0 \frac{1}{2} \int_0^\infty \frac{\rho^2 n_0^2 - r^2 n^2}{n^4(\rho + \zeta K)^3} \frac{1}{2n} \chi(\zeta) d\zeta; \quad (14)$$

$$\gamma_5 = \rho n_0 \frac{3}{8} \int_0^\infty \frac{(\rho^2 n_0^2 - r^2 n^2)^2}{n^6(\rho + \zeta K)^5} \frac{1}{2n} \chi(\zeta) d\zeta. \quad (15)$$

The associated bivariate power series of  $\gamma_1$  in terms of the small  $\chi_0$  and  $K/\rho$  is written down up to mixed third order in these two variables and integrated term-by-term:

$$\begin{aligned}
\gamma_1 &= \rho n_0 \frac{1}{2} \int_0^\infty \frac{1}{n^3(\rho + \zeta K)} \chi_0 e^{-\zeta} d\zeta \\
&= n_0 \chi_0 \frac{1}{2} \int_0^\infty \frac{1}{(1 + \chi_0 e^{-\zeta})^{3/2} (1 + \zeta K/\rho)} e^{-\zeta} d\zeta \\
&= n_0 \chi_0 \frac{1}{2} \int_0^\infty e^{-\zeta} \left[ 1 - \frac{3}{2} e^{-\zeta} \chi_0 - \zeta \frac{K}{\rho} + \frac{15}{8} e^{-2\zeta} \chi_0^2 + \frac{3}{2} \zeta e^{-\zeta} \chi_0 \frac{K}{\rho} + \zeta^2 \left(\frac{K}{\rho}\right)^2 \right. \\
&\quad \left. + \frac{35}{16} e^{-3\zeta} \chi_0^3 - \frac{15}{8} \zeta e^{-2\zeta} \chi_0^2 \frac{K}{\rho} - \frac{3}{2} \zeta^2 e^{-\zeta} \chi_0 \left(\frac{K}{\rho}\right)^2 - \zeta^3 \left(\frac{K}{\rho}\right)^3 \pm \dots \right] d\zeta \\
&= n_0 \chi_0 \frac{1}{2} \left[ 1 - \frac{3}{4} \chi_0 - \frac{K}{\rho} + \frac{5}{8} \chi_0^2 + \frac{3}{8} \chi_0 \frac{K}{\rho} + 2 \left(\frac{K}{\rho}\right)^2 - \frac{35}{64} \chi_0^3 - \frac{5}{24} \chi_0^2 \frac{K}{\rho} - \frac{3}{8} \chi_0 \left(\frac{K}{\rho}\right)^2 - 6 \left(\frac{K}{\rho}\right)^3 \pm \dots \right]. \quad (16)
\end{aligned}$$

This type of expansion as a power series of  $K/\rho$  is not new [13].

- In practise  $\chi_0$  is known not better than a relative accuracy of  $10^{-4}$ , and  $K/\rho$  is of the same magnitude; so keeping more than the first 3 terms in the square bracket in that expansion is a mere academic exercise from the point of view of an error budget.
- If gas mixtures of the air are treated as independent linear responses such that  $\chi_0$  is an additive composition proportional to the weighted contribution of the air components, this formula does obviously not apply beyond the first terms in the square bracket, because otherwise mixed quadratic terms of the individual  $\chi_0$  of the constituents interfere with the higher orders (App. A).
- At a precision of better than a milli-arcsecond, the oblate ellipsoidal Earth model introduces two different principal curvatures here that cause an azimuthal wobble of the azimuths [14].

For the third order in  $\tan z_0$  up to second mixed order

$$\begin{aligned}
\gamma_3 &= \rho n_0 \frac{1}{4} \int_0^\infty \frac{\rho^2 n_0^2 - (\rho + \zeta K)^2 n^2}{n^5 (\rho + \zeta K)^3} \chi_0 e^{-\zeta} d\zeta \\
&= n_0 \chi_0 \frac{1}{4} \int_0^\infty \frac{n_0^2 - (1 + \zeta K/\rho)^2 n^2}{(1 + \chi_0 e^{-\zeta})^{5/2} (1 + \zeta K/\rho)^3} e^{-\zeta} d\zeta; \\
&= n_0 \chi_0 \frac{1}{4} \left[ \frac{1}{2} \chi_0 - 2 \frac{K}{\rho} - \frac{5}{12} \chi_0^2 - \frac{3}{2} \chi_0 \frac{K}{\rho} + 10 \left(\frac{K}{\rho}\right)^2 \pm \dots \right] \quad (17)
\end{aligned}$$

For the fifth order in  $\tan z_0$  up to second mixed order

$$\begin{aligned}
\gamma_5 &= \rho n_0 \frac{3}{16} \int_0^\infty \frac{(\rho^2 n_0^2 - (\rho + \zeta K)^2 n^2)^2}{n^7 (\rho + \zeta K)^5} \chi_0 e^{-\zeta} d\zeta \\
&= n_0 \chi_0 \frac{3}{16} \int_0^\infty \frac{(n_0^2 - (1 + \zeta K/\rho)^2 n^2)^2}{(1 + \chi_0 e^{-\zeta})^{7/2} (1 + \zeta K/\rho)^5} e^{-\zeta} d\zeta \\
&= n_0 \chi_0 \frac{3}{16} \left[ \frac{1}{3} \chi_0^2 - 3 \chi_0 \frac{K}{\rho} + 8 \left(\frac{K}{\rho}\right)^2 \pm \dots \right]. \quad (18)
\end{aligned}$$

More  $\gamma_i$  coefficients are in the function `gamm` in the file `RefrExpo.cxx` in the source code.

The difference between including only  $\tan z_0$  and including all up to  $\tan^7 z_0$  is for example 0.8 arcsec (112.60 arcsec versus 111.79 arcsec) for  $z_0 = 70^\circ$  at  $\chi_0 = 4 \times 10^{-4}$  and  $K/\rho = 9.6/6380$ .

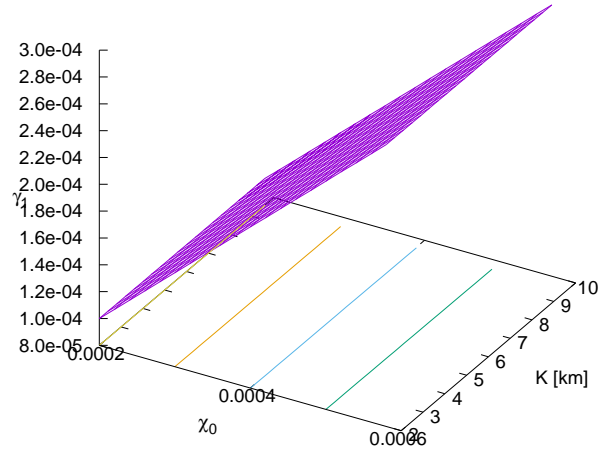


FIG. 2. The coefficient  $\gamma_1$  in radians as a function of  $\chi_0$  and  $K$  at  $\rho = 6380$  km. At this resolution there is almost no dependence on the scale height  $K$ , so  $\gamma_1 \approx n_0 \chi_0 / 2$ .  $2 \times 10^{-4}$  rad is equivalent to 41 arcsec at  $z_0 = 45^\circ$ .

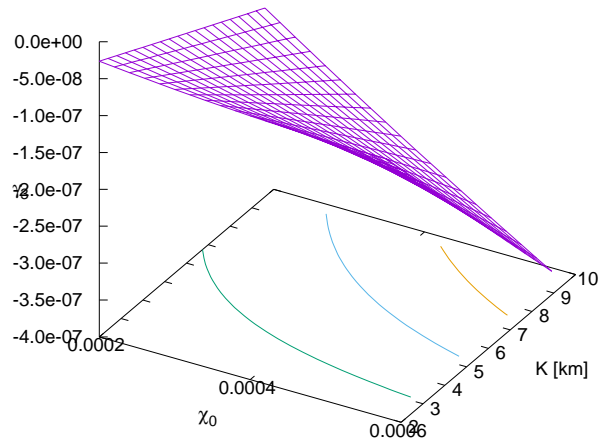


FIG. 3. The coefficient  $\gamma_3$  in radians as a function of  $\chi_0$  and  $K$  at  $\rho = 6380$  km.  $2 \times 10^{-7}$  rad are equivalent to 40 mas.

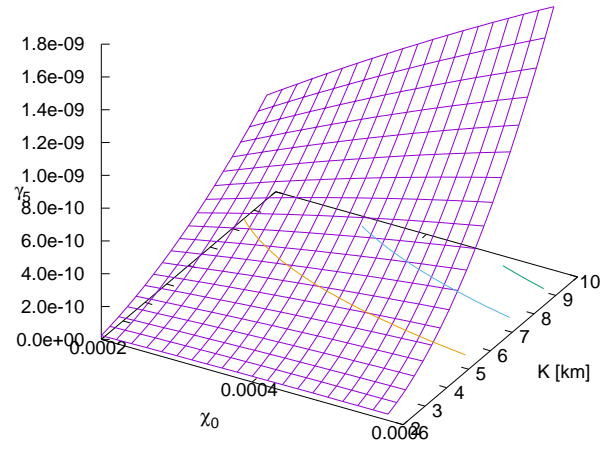


FIG. 4. The coefficient  $\gamma_5$  in radians as a function of  $\chi_0$  and  $K$  at  $\rho = 6380$  km.  $10^{-9}$  rad are equivalent to 0.2 mas.

### III. ACTIVE OPTICS ABERRATIONS

The implication of the previous section for telescope operation is that the telescope axis is corrected by a tilt  $R$  while acquiring an object at an astrometric zenith angle  $z$ . Which further imprint does the asymmetry of the global spherical atmosphere leave if the telescope's primary mirror collects light from a beam which does not have a perfect cylindrical symmetry because the radius of curvature of the atmosphere is not on the telescope axis? Which quasi-static aberrations beyond that type of 'lowest Zernike order' appear, and how much is the wavefront already bent as it hits the primary?

We answer this question quantitatively by representing the entrance pupil of the primary as a (continuous) set of baselines, with the same mathematical tools as for interferometric baselines [10].

#### A. Optical Path Length

In a global coordinate system centered at the Earth center, the star light is represented by a bundle of parallel rays approaching the Earth starting at very large values on the positive  $x$ -axis. (This does not restrict the results because we may tilt the Earth axis here such that the star is in the equatorial plane.) The center of the primary mirror has a distance  $\rho$  from the Earth center and is located at geodetic latitude  $\varphi$ ,

$$\vec{m}(0,0) = \rho \begin{pmatrix} \cos \varphi \\ 0 \\ \sin \varphi \end{pmatrix}. \quad (19)$$

The astrometric zenith angle  $z$  is  $z = \varphi$ , representing a direction  $(1,0,0)$  in the global coordinate system. The actual pointing axis of the telescope is along the zenith angle  $z_0 = \varphi - R$ , which is the direction  $(\cos R, 0, \sin R)$  in the global coordinate system. The points in the entrance pupil of the primary mirror have local coordinates  $m_{x,y}$  where  $m_h$  points along the local horizontal and  $m_v$  from the center to the upper rim, and where  $m_h^2 + m_v^2$  is smaller than the squared radius of the primary.

The task is to calculate the optical path length

$$L = \int_{n=1}^{n=n_0} n \frac{dr}{\cos \psi}, \quad (20)$$

the air mass weighted with the refractive index, given  $m_h$  and  $m_v$  in the entrance pupil, or, more precisely, recovering the differential optical path length relative to the center. This becomes a mixed boundary problem: we define locations of the rays in the entrance pupil, but directions (their tilts, derivatives) at some common virtual entrance pupil high above the atmosphere.

#### B. Spanning the Entrance Pupil

The global position of a point in the circular entrance pupil is the center of the pupil plus two components perpendicular to the pointing direction  $z_0(0,0)$  with lengths  $m_h$  and  $m_v$ :

$$\vec{m}(m_h, m_v) = \vec{m}(0,0) + m_v \begin{pmatrix} -\sin R(0,0) \\ 0 \\ \cos R(0,0) \end{pmatrix} + m_h \begin{pmatrix} 0 \\ 1 \\ 0 \end{pmatrix} = \begin{pmatrix} \rho(0,0) \cos z(0,0) - m_v \sin R(0,0) \\ m_h \\ \rho(0,0) \sin \varphi + m_v \cos R(0,0) \end{pmatrix}. \quad (21)$$

The zenith angles  $z$  and  $z_0$ , the refractive indices  $n$  and  $\chi_0$ , and the distances  $\rho$  and  $r$  to the Earth center are functions of the  $(m_h, m_v)$  coordinates of the pupil coordinates. The refinement of Figure 1 for a bundle of rays which enter from the right leads to Figure 5.

The distance of such a point to the Earth center is  $|\vec{m}|$  and defines the variation of the local refractive index due to the variation of the air density in the entrance pupil:

$$|\vec{m}(m_h, m_v)| = \rho(m_h, m_v) = \sqrt{\rho^2(0,0) + m_h^2 + m_v^2 + 2\rho(0,0)m_v \sin z_0(0,0)}. \quad (22)$$

The direction of the zenith of these points in the entrance pupil is  $\vec{m}/|\vec{m}|$ , defined as to split the entrance pupil into smaller areas which share a common pointing axis but which collect light that is bent along individual curved paths.

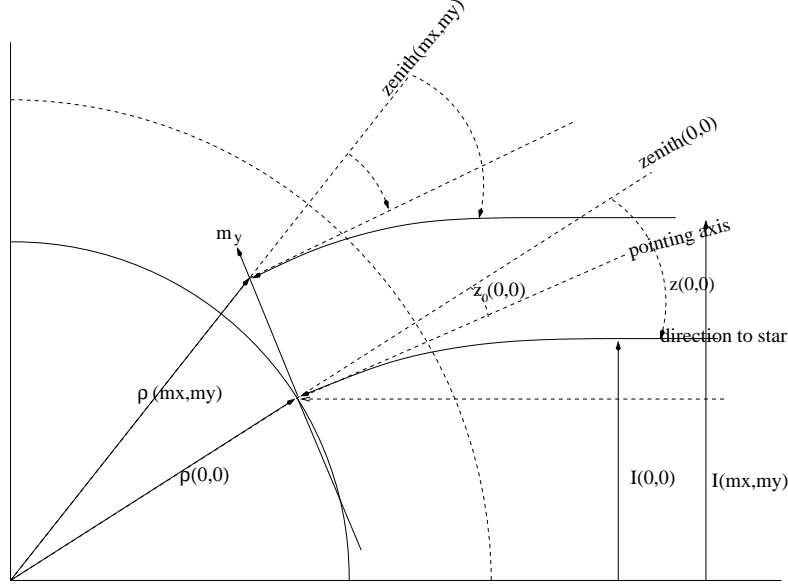


FIG. 5. The telescope points into a direction described by  $z_0(0,0)$ .  $m_h$  (not shown, pointing into the drawing plane) and  $m_v$  are directions orthogonal to that pointing direction. Two bent rays from a common star run parallel high above the atmosphere and reach the pupil with two different sets of zenith angles  $z$ ,  $z_0$ , impact parameters  $I$ , and air densities  $\chi$ . Not to scale.

The astrometric zenith angles  $z(m_h, m_v)$  of points in the entrance pupil are aligned (above the atmosphere) to a common direction; by building the dot product of  $\vec{m}/|\vec{m}|$  with the vector of the incoming light,  $z$  is computed from

$$\cos z(m_h, m_v) = \frac{1}{|\vec{m}(m_h, m_v)|} [\rho(0,0) \cos z - m_v \sin R(0,0)]. \quad (23)$$

This is inconvenient because the application further down is formulated in terms of the true zenith angle  $z_0(m_h, m_v)$ . To obtain  $z_0(m_h, m_v)$  we may

- recompute  $R$  in terms of  $\tan z$  as demonstrated in [10],
- or solve (1),  $z - z_0 = \sum_{i=1,3,5,\dots} \gamma_i \tan^i z_0$ , for  $z_0$  via a few iterations of a Newton method:

$$z_0^{(j)} = z_0^{(j-1)} - \frac{z_0 - z + \sum_{i=1,3,5,\dots} \gamma_i \tan^i z_0^{(j-1)}}{1 + \sum_{i=1,3,5,\dots} i \gamma_i \tan^{(i-1)} z_0^{(j-1)} [1 + \tan^2 z_0^{(j-1)}]}, \quad (24)$$

starting with a first estimate  $z_0^{(0)} = z$ .

Each point in the entrance pupil has a path length  $L(m_h, m_v)$  of a ray that terminates there. Rephrasing (20) with the Fresnel law (see [10]) gives

$$L = \int_{n=1}^{n=n_0} r n^2 \frac{dr}{\sqrt{n^2 r^2 - n_0^2 \rho^2 \sin^2 z_0}}. \quad (25)$$

The aberration across the pupil, measured in length units, is the path length difference between a ray that ends at a general point and a ray that ends at the center:

$$\Delta L = \int_{n=1}^{n=n_0(m_h, m_v)} r n^2 \frac{dr}{\sqrt{n^2 r^2 - n_0(m_h, m_v)^2 \rho(m_h, m_v)^2 \sin^2 z_0(m_h, m_v)}} - \int_{n=1}^{n=n_0(0,0)} r n^2 \frac{dr}{\sqrt{n^2 r^2 - n_0(0,0)^2 \rho(0,0)^2 \sin^2 z_0(0,0)}}. \quad (26)$$

### C. Series Expansions

The first integral may be split by prolonging the ray to the atmospheric layer of the center and by backing up from there to the layer in the pupil:

$$\begin{aligned} \Delta L = & \int_{n=1}^{n=n_0(0,0)} rn^2 \frac{dr}{\sqrt{n^2 r^2 - n_0(m_h, m_v)^2 \rho(m_h, m_v)^2 \sin^2 z_0(m_h, m_v)}} \\ & + \int_{n=n_0(0,0)}^{n=n_0(m_h, m_v)} rn^2 \frac{dr}{\sqrt{n^2 r^2 - n_0(m_h, m_v)^2 \rho(m_h, m_v)^2 \sin^2 z_0(m_h, m_v)}} \\ & - \int_{n=1}^{n=n_0(0,0)} rn^2 \frac{dr}{\sqrt{n^2 r^2 - n_0(0,0)^2 \rho(0,0)^2 \sin^2 z_0(0,0)}}. \end{aligned} \quad (27)$$

Define impact parameters  $I$

$$I(m_h, m_v) \equiv n_0(m_h, m_v) \rho(m_h, m_v) \sin z_0(m_h, m_v). \quad (28)$$

The aberration is split into a contribution of the second integral and a compound term of the first and third integral,  $\Delta L = \Delta L^{(1)} + \Delta L^{(2)}$ . The second integral is rephrased as a function of the variables of Section III:

$$\begin{aligned} \Delta L^{(1)} = & \int_{n=n_0(0,0)}^{n=n_0(m_h, m_v)} rn^2 \frac{dr}{\sqrt{n^2 r^2 - I^2(m_h, m_v)}} = \int_{r=\rho(0,0)}^{r=\rho(m_h, m_v)} r(1+\chi) \frac{dr}{\sqrt{(1+\chi)r^2 - I^2(m_h, m_v)}} \\ = & K \int_{\zeta=0}^{\zeta=\zeta(m_h, m_v)} (1+\zeta K/\rho)(1+\chi_0 e^{-\zeta}) \frac{d\zeta}{\sqrt{(1+\chi_0 e^{-\zeta})(1+\zeta K/\rho)^2 - I^2(m_h, m_v)/\rho^2}}. \end{aligned} \quad (29)$$

This is expanded in a bivariate power series for small  $\chi_0$  and  $K/\rho$ :

$$\begin{aligned} \Delta L^{(1)} = & K \int_{\zeta=0}^{\zeta=\zeta(m_h, m_v)} \left[ \frac{1}{(1-\hat{I}^2)^{1/2}} - \frac{\hat{I}^2}{(1-\hat{I}^2)^{3/2}} \zeta \frac{K}{\rho} + \frac{1}{2} \frac{1-2\hat{I}^2}{(1-\hat{I}^2)^{3/2}} e^{-\zeta} \chi_0 + \frac{3}{2} \frac{\hat{I}^2}{(1-\hat{I}^2)^{5/2}} \zeta^2 \left(\frac{K}{\rho}\right)^2 \right. \\ & + \frac{1}{2} \frac{\hat{I}^2(1+2\hat{I}^2)}{(1-\hat{I}^2)^{5/2}} \zeta e^{-\zeta} \frac{K}{\rho} \chi_0 - \frac{1}{8} \frac{\hat{I}-4\hat{I}^2}{(1-\hat{I}^2)^{5/2}} e^{-2\zeta} \chi_0^2 \\ & - \frac{1}{2} \frac{\hat{I}^2(4+\hat{I}^2)}{(1-\hat{I}^2)^{7/2}} \zeta^3 \left(\frac{K}{\rho}\right)^3 - \frac{3}{4} \frac{\hat{I}^2(1+4\hat{I}^2)}{(1-\hat{I}^2)^{7/2}} \zeta^2 e^{-\zeta} \left(\frac{K}{\rho}\right)^2 \chi_0 \\ & \left. - \frac{3}{8} \frac{\hat{I}^2(1+4\hat{I}^2)}{(1-\hat{I}^2)^{7/2}} \zeta e^{-2\zeta} \frac{K}{\rho} \chi_0^2 + \frac{1}{16} \frac{1-6\hat{I}^2}{(1-\hat{I}^2)^{7/2}} e^{-3\zeta} \chi_0^3 + \dots \right] d\zeta \end{aligned} \quad (30)$$

where  $\chi_0 = \chi_0(0,0)$ ,  $\rho = \rho(0,0)$  and  $\hat{I} \equiv I(m_h, m_v)/\rho$ . Term-by-term integration yields

$$\begin{aligned} \Delta L^{(1)} = & K \left[ \frac{1}{(1-\hat{I}^2)^{1/2}} \zeta - \frac{1}{2} \frac{\hat{I}^2}{(1-\hat{I}^2)^{3/2}} \zeta^2 \frac{K}{\rho} - \frac{1}{2} \frac{1-2\hat{I}^2}{(1-\hat{I}^2)^{3/2}} e^{-\zeta} \chi_0 + \frac{1}{2} \frac{\hat{I}^2}{(1-\hat{I}^2)^{5/2}} \zeta^3 \left(\frac{K}{\rho}\right)^2 \right. \\ & - \frac{1}{2} \frac{\hat{I}^2(1+2\hat{I}^2)}{(1-\hat{I}^2)^{5/2}} (1+\zeta) e^{-\zeta} \frac{K}{\rho} \chi_0 + \frac{1}{16} \frac{\hat{I}-4\hat{I}^2}{(1-\hat{I}^2)^{5/2}} e^{-2\zeta} \chi_0^2 \\ & - \frac{1}{8} \frac{\hat{I}^2(4+\hat{I}^2)}{(1-\hat{I}^2)^{7/2}} \zeta^4 \left(\frac{K}{\rho}\right)^3 + \frac{3}{4} \frac{\hat{I}^2(1+4\hat{I}^2)}{(1-\hat{I}^2)^{7/2}} (2+2\zeta+\zeta^2) e^{-\zeta} \left(\frac{K}{\rho}\right)^2 \chi_0 \\ & \left. + \frac{3}{32} \frac{\hat{I}^2(1+4\hat{I}^2)}{(1-\hat{I}^2)^{7/2}} (1+2\zeta) e^{-2\zeta} \frac{K}{\rho} \chi_0^2 - \frac{1}{48} \frac{1-6\hat{I}^2}{(1-\hat{I}^2)^{7/2}} e^{-3\zeta} \chi_0^3 + \dots \right]_{\zeta=0}^{\zeta(m_h, m_v)}. \end{aligned} \quad (31)$$

More terms are listed in the function `deltaL1Int` in the file `M1aberr.cxx` in the source code.

The first and third term of (27) are expanded in powers of  $\Delta I \equiv I(0,0) - I(m_h, m_v)$ , which is of the order of the pupil radius because the atmosphere is thin:

$$\frac{1}{\sqrt{n^2 r^2 - I^2(m_h, m_v)}} - \frac{1}{\sqrt{n^2 r^2 - I^2(0,0)}} = -\frac{I(m_h, m_v)}{(n^2 r^2 - I(m_h, m_v))^{3/2}} \Delta I$$

$k$	$c$	$i$	$\alpha$
0	1	1	$-\frac{\hat{I}(1+2\hat{I}^2)}{2}$
0	1	2	$-\frac{1+10\hat{I}^2+4\hat{I}^4}{4}$
0	1	3	$-\frac{(9+22\hat{I}^2+4\hat{I}^4)\hat{I}}{4}$
1	1	1	$\frac{(2+11\hat{I}^2+2\hat{I}^4)\hat{I}}{4}$
1	1	2	$\frac{2+45\hat{I}^2+54\hat{I}^4+4\hat{I}^6}{2}$
1	1	3	$\frac{(36+177\hat{I}^2+98\hat{I}^4+4\hat{I}^6)\hat{I}}{4}$
0	2	1	$\frac{3(1+4\hat{I}^2)\hat{I}}{16}$
0	2	2	$\frac{3+54\hat{I}^2+48\hat{I}^4}{32}$
0	2	3	$\frac{5(9+38\hat{I}^2+12\hat{I}^4)\hat{I}}{32}$
2	1	1	$-\frac{3(2+21\hat{I}^2+12\hat{I}^4)\hat{I}}{2}$

TABLE I.  $\alpha$ -coefficients of Eq. (35) for small powers of the three expansion coefficients.

$$\begin{aligned}
& -\frac{1}{2} \frac{n^2 r^2 + 2I^2(m_h, m_v)}{(n^2 r^2 - I(m_h, m_v))^{5/2}} (\Delta I)^2 \\
& -\frac{3}{2} \frac{[3n^2 r^2 + 2I^2(m_h, m_v)]I(m_h, m_v)}{(n^2 r^2 - I(m_h, m_v))^{7/2}} (\Delta I)^3 \\
& -\frac{1}{8} \frac{3n^4 r^4 + 24n^2 r^2 I^2(m_h, m_v) + 8I^4(m_h, m_v)}{(n^2 r^2 - I(m_h, m_v))^{9/2}} (\Delta I)^4 + \dots
\end{aligned} \tag{32}$$

$$\begin{aligned}
\Delta L^{(2)} &= \int_{r=\infty}^{\rho(0,0)} dr \left[ \frac{rn^2}{\sqrt{n^2 r^2 - I^2(m_h, m_v)}} - \frac{rn^2}{\sqrt{n^2 r^2 - I^2(0, 0)}} \right] \\
&= K \int_{\zeta=\infty}^0 d\zeta \left[ -\frac{(1 + \zeta K/\rho)(1 + \chi_0 e^{-\zeta})\hat{I}}{(n^2 r^2 - \hat{I})^{3/2}} (\Delta I)/\rho \right. \\
&\quad -\frac{1}{2} \frac{(1 + \zeta K/\rho)n^2[n^2(1 + \zeta K/\rho)^2 + 2\hat{I}^2]}{(n^2 r^2 - \hat{I})^{5/2}} (\Delta I/\rho)^2 \\
&\quad -\frac{3}{2} \frac{(1 + \zeta K/\rho)n^2[3n^2(1 + \zeta K/\rho)^2 + 2\hat{I}^2]\hat{I}}{(n^2 r^2 - \hat{I})^{7/2}} (\Delta I/\rho)^3 \\
&\quad \left. -\frac{1}{8} \frac{(1 + \zeta K/\rho)n^2[3n^4(1 + \zeta K/\rho)^4 + 24n^2(1 + \zeta K/\rho)^2\hat{I}^2 + 8\hat{I}^4]}{(n^2 r^2 - \hat{I})^{9/2}} (\Delta I/\rho)^4 + \dots \right].
\end{aligned} \tag{33}$$

In a double expansion in orders of  $K/\rho$  and  $\chi_0$ , we integrate the orders of  $\chi_0^0$  all in once:

$$\begin{aligned}
\Delta L^{(2)} \xrightarrow{\chi_0 \rightarrow 0, n \rightarrow 1} & \int_{r=\infty}^{\rho(0,0)} dr \left[ \frac{r}{\sqrt{r^2 - I^2(m_h, m_v)}} - \frac{r}{\sqrt{r^2 - I^2(0, 0)}} \right] \\
&= \sqrt{\rho^2 - I^2(m_h, m_v)} - \sqrt{\rho^2 - I^2(0, 0)}.
\end{aligned} \tag{34}$$

The full expansion in powers of  $K/\rho$ ,  $\chi_0$  and  $\Delta I/\rho$  can then be written as

$$\Delta L^{(2)} = \sqrt{\rho^2 - I^2(m_h, m_v)} - \sqrt{\rho^2 - I^2(0, 0)} + K \sum_{k \geq 0} \sum_{c \geq 1} \sum_{i \geq 1} \alpha_{k,c,i} (K/\rho)^k \chi_0^c (\Delta I/\rho)^i \frac{1}{(1 - \hat{I}^2)^{1/2+k+c+i}}. \tag{35}$$

where  $K/\rho$  is of the order of 10 kilometers over the Earth radius,  $\chi_0$  is of the order of a few  $\times 10^{-4}$  for typical optical telescopes, and where  $\Delta I/\rho$  is of the order of the primary mirror radius over the Earth radius. Some  $\alpha_{k,c,i}$  are tabulated in Table I; a more complete set is in the function `deltaL2Series` in the file `M1aberr.cxx` of the source code.

#### D. Numerical Example

The result for prototypical E-ELT variables is shown in Figure 6: With Ciddor's formulas for the index of refraction we assume a wavelength of 500 nm, a temperature of 10° C, a pressure of 697 hPa, a CO<sub>2</sub> content of 470 ppm, so

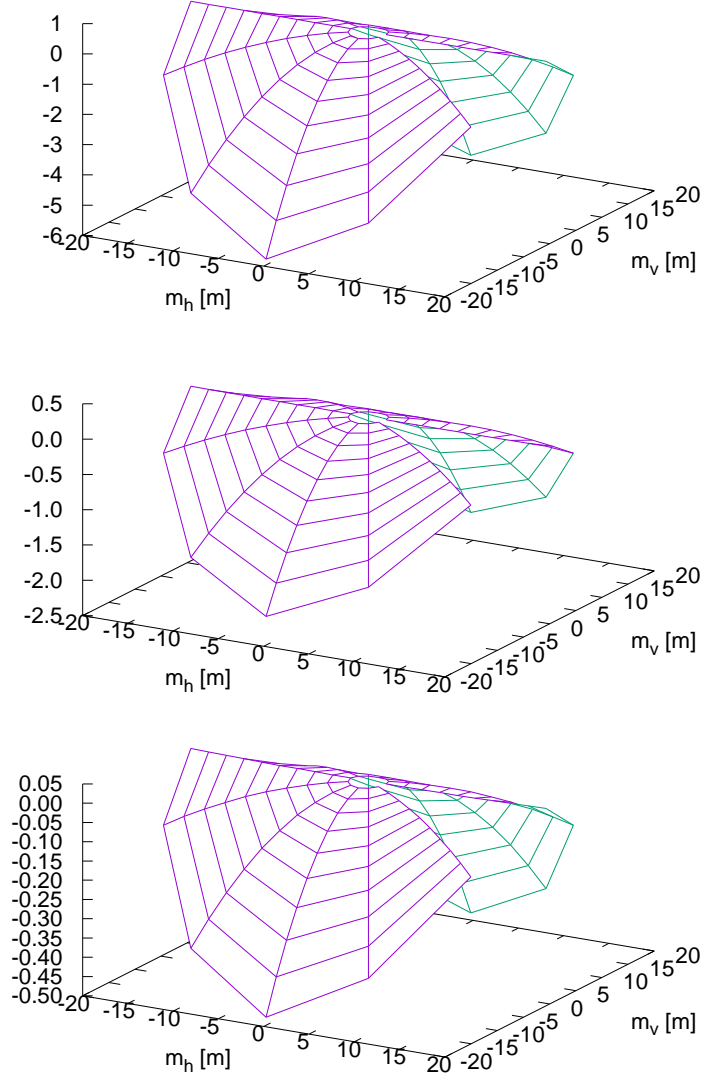


FIG. 6. The optical path length difference  $\Delta L$  in microns in the entrance pupil of a 40-m telescope for zenith angles of 60 (top), 40 (middle) and 20 degrees (bottom) at  $\chi_0 = 3.9 \times 10^{-4}$ .

the refractive index is 1.000195229, and  $\chi_0 = 3.9 \times 10^{-4}$ . The semi-major axis and flattening of the WGS84 [8] at a geographic latitude of  $\varphi = 24^\circ 35'$ , and sea level altitude 3046 m gives a distance  $\rho(0, 0) = 6377.5$  km to the Earth center. Results are plotted for a radius up to  $\sqrt{m_h^2 + m_v^2} \leq 19.6$  m and a scale height of  $K = 9600$  m. The conclusion is:

- There is almost no residual optical path length along the horizontal ( $m_h$ ) axis (tip).
- There is essentially no tilt component left, which means a tilt of the telescope axis by  $R$  as computed in Section II removes the first-order Zernike terms, as expected.
- The residual difference of the path length of the upper and lower rim ( $m_v$ ) relative to the center is up to  $6 \mu\text{m}$  of uni-axial defocus at a zenith distance of  $60^\circ$ .

We may zoom into such a graph and plot the absolute value of  $\Delta L$  in a cut from the center of the pupil to the upper rim, which yields Figure 7. This plot with a double logarithmic scale of the optical path difference shows that

- the functions are almost straight lines for zenith distances up to  $60^\circ$ ; the aberration is approximately proportional

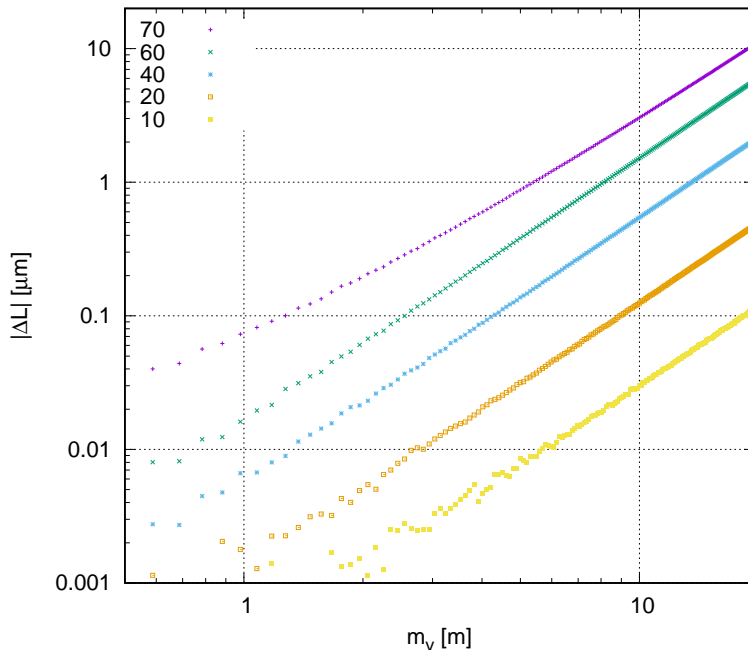


FIG. 7. The absolute value of optical path length difference  $\Delta L$  in microns in the entrance pupil between the upper rim and the center for zenith angles of 70, 60, 40, 20 and 10 degrees (top to bottom). These are cuts through graphs of Figure 6 at  $m_h = 0$ .

to the squared distance (not a pure second-order Zernike term). For a 8m-telescope at  $z = 60^\circ$  the path difference is only  $0.26 \mu\text{m}$ .

- the numerical implementation has jitters on path length scales of typically 5 nanometers. This is likely a consequence of rounding errors with the double-precision arithmetics in the C++ source code, plus precision limits caused by cut-offs in the number of Taylor terms included while computing  $\Delta L^{(1)}$  and  $\Delta L^{(2)}$ .

In a general telescope operation effects of the order calculated here are probably not observed, because a focusing model that includes flexure compensations or wind loads as a function of zenith angle must handle basically the same data.

With another cut through the parameter set we may keep  $z_0$  and  $m_v$  fixed and look at  $\Delta L$  as a function of the refractive index at the ground; this is relevant if the adaptive optics system and the science cameras observe at different wavelengths and hence at different  $\chi_0$ . The numerical data of Figure 8 reveal that the change in  $\Delta L$  is practically proportional to  $\chi_0$  as long as the scale height is fixed. In consequence one may map relative differential chromatic differences in the susceptibilities directly to relative differential aberrations in the entrance pupil.

#### IV. SUMMARY

In a barometric exponential model of the the air susceptibility profile above the telescope we presented approximate analytical formulas

1. of the differential zenith angle  $R$  as a power series of the tangent of the zenith angle with expansion coefficients summarized in (16), (17) and (18);
2. of the path length distribution  $\Delta L$  of rays in the entrance pupil with two contributions summarized by (31) and (35).

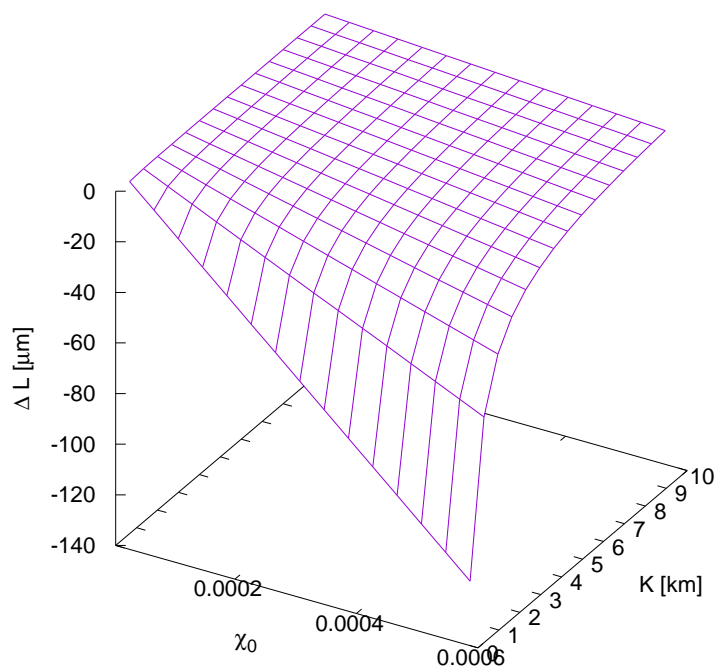


FIG. 8. The optical path length difference  $\Delta L$  in microns in the entrance pupil at the upper rim 19.6m away from the center for a zenith angle of  $60^\circ$ .

### Appendix A: Segregated Scale Heights

If gas mixtures of the air are treated as independent linear responses such that  $\chi_0$  is an additive composition proportional to the weighted contribution of the air components, Equation (16) breaks already in the first three terms in the square brackets if the scale heights of the molecular constituents differ. The typical case is an additive mixture of dry air and water vapor, where dry air has a scale height  $K$  near 9 kilometers, but water vapor disappears at a scale height of approximately 2 kilometers [15–18]. To illustrate that variant, one would introduce a susceptibility with two scale heights  $K_1$  and  $K_2$ ,

$$\chi(r) = \chi_{01}e^{-(r-\rho)/K_1} + \chi_{02}e^{-(r-\rho)/K_2} = \chi_{01}e^{-(r-\rho)/K_1} + (1 \leftrightarrow 2), \quad (\text{A1})$$

where  $1 \leftrightarrow 2$  means the previous terms is repeated where the roles of  $K_1$  and  $K_2$  are swapped, and also the roles of  $\chi_{01}$  and  $\chi_{02}$  are swapped. The lowest order expansion for small  $\hat{K}_1 \equiv K_1/\rho$  and  $\hat{K}_2 \equiv K_2/\rho$  and small  $\chi_{01}, \chi_{02}$  is

$$\begin{aligned} \gamma_1 &= \frac{1}{2}\rho n_0 \int_1^{n_0} \frac{1}{n^3 r} d\chi \\ &= \frac{1}{2}\rho n_0 \int_\rho^\infty \frac{1}{[1 + \chi_{01}e^{-(r-\rho)/K_1} + \chi_{02}e^{-(r-\rho)/K_2}]^{3/2} r} \left[ \frac{1}{K_1} \chi_{01}e^{-(r-\rho)/K_1} + \frac{1}{K_2} \chi_{02}e^{-(r-\rho)/K_2} \right] dr \\ &= \frac{1}{2}\rho n_0 \int_0^\infty \frac{1}{[1 + \chi_{01}e^{-r/K_1} + \chi_{02}e^{-r/K_2}]^{3/2} (r + \rho)} \left[ \frac{1}{K_1} \chi_{01}e^{-r/K_1} + \frac{1}{K_2} \chi_{02}e^{-r/K_2} \right] dr \\ &= \frac{1}{2} \frac{\rho}{K_1} n_0 \chi_{01} \int_0^\infty \frac{e^{-r/K_1}}{[1 + \chi_{01}e^{-r/K_1} + \chi_{02}e^{-r/K_2}]^{3/2} (r + \rho)} dr + (1 \leftrightarrow 2) \\ &\approx \frac{\chi_{01}}{8(\hat{K}_1 + \hat{K}_2)} \left[ 4(\hat{K}_1 + \hat{K}_2 - \hat{K}_1\hat{K}_2 - \hat{K}_1^2) + 2\chi_{02}\hat{K}_1 - 4\chi_{02}\hat{K}_2 - \chi_{01}(\hat{K}_1 + \hat{K}_2) \right] + (1 \leftrightarrow 2). \end{aligned} \quad (\text{A2})$$

### Appendix B: Cassini's model

The Cassini model of a homogeneous single-layer atmosphere of height  $h$  leads to a difference between observed and astrometric zenith angles of [19, §9.5]

$$R^{(C)} = \arcsin\left(\frac{n_0\rho \sin z_0}{\rho + h}\right) - \arcsin\left(\frac{\rho \sin z_0}{\rho + h}\right). \quad (\text{B1})$$

The bivariate Taylor expansion in orders of  $n_0 - 1$  and  $q$  starts

$$\begin{aligned} R^{(C)} &= (n_0 - 1) \tan z_0 \left[ 1 - \frac{q}{\cos^2 z_0} + \frac{1}{2}(n_0 - 1) \tan^2 z_0 + \frac{1}{2} \frac{q^2(3 - \cos^2 z_0)}{\cos^4 z_0} - \frac{3}{2} \frac{(n_0 - 1)q \tan^2 z_0}{\cos^2 z_0} \right. \\ &\quad \left. + \frac{1}{6} \frac{(n_0 - 1)^2 \tan^2 z_0 (3 - 2 \cos^2 z_0)}{\cos^2 z_0} + \dots \right] \end{aligned} \quad (\text{B2})$$

where  $q = h/\rho$ . The small difference  $R - R^{(C)}$  for a parameter set of  $\rho = 6377.36$  km,  $h = K = 6.82$  km and  $n_0 = 1.000284$  is illustrated in Figure 9.

One may expand  $R^{(C)}$  in powers of  $\tan z_0$ :

$$R^{(C)} = \sum_{i=1,3,5,\dots} \gamma_i^{(C)} \tan^i z_0, \quad (\text{B3})$$

such that

$$\gamma_1^{(C)} = n_0 \chi_0 \frac{1}{2} \left[ 1 - \frac{3}{4} \chi_0 - q + \frac{5}{8} \chi_0^2 + \frac{3}{4} \chi_0 q + q^2 + \dots \right], \quad (\text{B4})$$

$$\gamma_3^{(C)} = n_0 \chi_0 \frac{1}{4} \left[ \frac{1}{2} \chi_0 - 2q - \frac{5}{12} \chi_0^2 + 5q^2 + \dots \right]. \quad (\text{B5})$$

So the difference between the Cassini model and the exponential model (16) and (17) is

$$R - R^{(c)} \approx \frac{1}{2} n_0 \chi_0 \tan z_0 \left( -\frac{3}{4} \chi_0 q + q^2 + \dots \right) + \frac{1}{4} n_0 \chi_0 \tan^3 z_0 \left( -\frac{3}{2} \chi_0 q + 5q^2 + \dots \right) + \dots \quad (\text{B6})$$

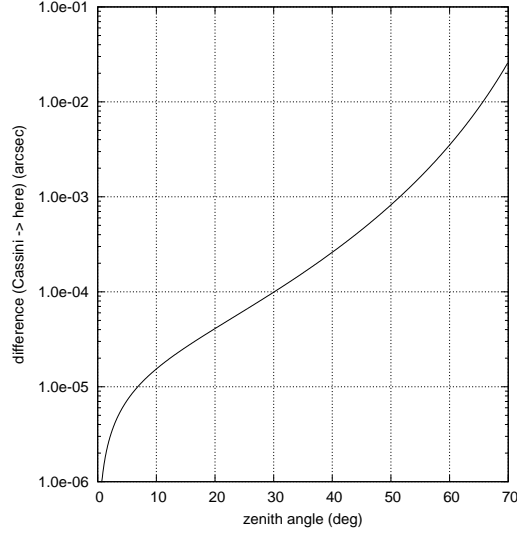


FIG. 9. The difference between the refraction predicted by (B1) and the model of exponential slope,  $R - R^{(C)}$ , as a function of zenith distance with  $n_0 = 1.000568081$  and  $\rho = 6377.36$  km and  $K = 6.82$  km.

## Appendix C: C++ implementation

### 1. Differential zenith angle

A C++ program to compute  $R$  as a function of  $\chi_0$  and  $K/\rho$  up to the order  $\tan^7 z_0$  with up to mixed 5th order for  $\tan z_0$  and up to mixed 4th order for  $\tan^3 z_0$ ,  $\tan^5 z_0$  and  $\tan^7 z_0$  is in the `anc` directory. The source files are `r.cxx`, `RefrExpo.cxx` and `RefrExpo.h`. The program is compiled with

```
g++ -o r -O2 r.cxx RefrExpo.cxx
```

or

```
make
```

and is run with up to 4 options:

```
r [-C] [-c chi0] [-K K] [-r rho]
```

where `chi0` is the value of  $\chi_0$  at the telescope site, `K` is the scale height in meters, and `rho` is the sum of the Earth radius and telescope sea level altitude in meters. The switch `-C` produces results with Cassini's model, using `K` for the layer height and `rho` for the earth radius. The program produces a table of  $z_0$  in degrees and values of  $R$  in arcseconds.

### 2. Input Pupil Aberration

Another C++ program to compute  $\Delta L$  as a function of  $\chi_0$ ,  $K$ ,  $\rho$ ,  $m_h$  and  $m_v$  is also attached. Source files are named `raberr.cxx`, `RefrExpo.cxx`, `RefrExpo.h`, `M1aberr.cxx` and `M1aberr.h`; it is compiled with

```
g++ -o raberr -O2 raberr.cxx RefrExpo.cxx M1aberr.cxx
```

or

```
make
```

and is run with

```
raberr [-c chi0] [-K K] [-r rho] [-R radius] [-1 Nsteps] -z zenith
```

where `chi0`, `K` and `rho` have the same meaning as above, where `radius` is the entrance pupil (primary) radius in meters, and where `zenith` is the zenith angle in degrees.

If the option `-1` is not used, it generates a table with three values per line suitable to create Figure 6:  $m_h$  and  $m_v$  in meters along concentric circles of the azimuth of the entrance pupil, and  $\Delta L$  in micrometers.

If the option `-1` is used, it generates a table with two values per line suitable to create Figure 7:  $m_v$  in meters for positive  $m_v$  and  $|\Delta L|$  in micrometers. `Nsteps` is the number of points on the  $m_v$  axis with a maximum set by `radius`.

- 
- [1] A. I. Mahan, *Appl. Opt.* **1**, 497 (1962).
  - [2] R. M. Green, *Spherical Astronomy* (Cambridge University Press, Cambridge, London, 1985).
  - [3] M. E. Thomas and R. I. Joseph, *Johns Hopkins Apl. Technical Digest* **17**, 279 (1996).
  - [4] L. H. Auer and E. M. Standish, *Astron. J.* **119**, 2472 (2000).
  - [5] B. D. Nener, N. Fowkes, and L. Borredon, *J. Opt. Soc. Am. A* **20**, 867 (2003).
  - [6] P. D. Noerdlinger, *ISPRS J. Photogr. Rem. Sens.* **54**, 360 (1999).
  - [7] C. Tannous and J. Nigrin, arXiv:physics/0104004 (2001), arxiv:physics/0104004.
  - [8] National Imagery and Mapping Agency, *Department Of Defense World Geodetic System 1984*, Tech. Rep. TR8350.2 (NIMA, 2000).
  - [9] R. C. Stone, *Publ. Astron. Soc. Pac.* **114**, 1070 (2002).
  - [10] R. J. Mathar, *Baltic Astronomy* **14**, 277 (2005).
  - [11] M. N. Berberan-Santos, E. N. Bodunov, and L. Pogliani, *Am. J. Phys.* **65**, 404 (1997).
  - [12] J. B. West, *J. Appl. Physiology* **81**, 1850 (1996).
  - [13] M. Eshagh, *Artif. Satel.* **43**, 25 (2008).
  - [14] R. J. Mathar, arXiv:0907.1104 [astro-ph.IM] (2009), arXiv:0907.1104.
  - [15] D. D. Turner, R. A. Ferrare, and L. A. Brasseur, *Geophys. Res. Lett.* **28**, 4441 (2001).
  - [16] C. Cahen, G. Megie, and P. Flamant, *J. Appl. Meteorol.* **21**, 1506 (1982).
  - [17] K. Parameswaran and B. V. K. Murthy, *J. Appl. Meteorol.* **29**, 665 (1990).
  - [18] A. Otárola, T. Travouillon, M. Schöck, S. Els, R. Riddle, W. Skidmore, R. Dahl, D. Naylor, and R. Querel, *Publ. Astron. Soc. Pac.* **122**, 470 (2010).
  - [19] A. T. Young, *Astron. J.* **127**, 3622 (2004).